

Phase behavior of polydisperse sticky hard spheres: analytical solutions and perturbation theory

Domenico Gazzillo, Riccardo Fantoni & Achille Giacometti *

Istituto Nazionale per la Fisica della Materia and Dipartimento di Chimica Fisica, Università di Venezia, S. Marta
DD 2137, I-30123 Venezia, Italy
(v3.2 released August 2005)

We discuss phase coexistence of polydisperse colloidal suspensions in the presence of adhesion forces. The combined effect of polydispersity and Baxter's sticky-hard-sphere (SHS) potential, describing hard spheres interacting via strong and very short-ranged attractive forces, give rise, within the Percus-Yevick (PY) approximation, to a system of coupled quadratic equations which, in general, cannot be solved either analytically or numerically. We review and compare two recent alternative proposals, which we have attempted to by-pass this difficulty. In the first one, truncating the density expansion of the direct correlation functions, we have considered approximations simpler than the PY one. These C_n approximations can be systematically improved. We have been able to provide a complete analytical description of polydisperse SHS fluids by using the simplest two orders C_0 and C_1 , respectively. Such a simplification comes at the price of a lower accuracy in the phase diagram, but has the advantage of providing an analytical description of various new phenomena associated with the onset of polydispersity in phase equilibria (e.g. fractionation). The second approach is based on a perturbative expansion of the polydisperse PY solution around its monodisperse counterpart. This approach provides a sound approximation to the real phase behavior, at the cost of considering only weak polydispersity. Although a final settlement on the soundness of the latter method would require numerical simulations for the polydisperse Baxter model, we argue that this approach is expected to keep correctly into account the effects of polydispersity, at least qualitatively.

1 Introduction

New technological advances in physico-chemical manipulation of colloidal mixtures have brought up again the issue of theoretically understanding the phase behaviour of polydisperse systems (1). 'Polydispersity' in colloidal solutions means that, due to their production process, suspended macroparticles with the same chemical composition cannot be exactly identical to each other, but in general have different sizes, and possibly different surface charges, shapes, etc. In practice, a polydisperse system can be reckoned as a mixture with very large – or essentially infinite – number M of different species or components, identified by one or several parameters (M large but finite refers to *discrete polydispersity*, whereas $M \rightarrow \infty$ with a continuous distribution of polydisperse parameters corresponds to *continuous polydispersity*). The present paper will consider discrete polydispersity of spherical colloidal particles, with their diameter being the only polydisperse attribute (size-polydispersity).

When polydispersity is not negligible, the phase behaviour becomes much richer, but the determination of phase transition boundaries requires a much more involved formalism, compared to the monodisperse counterpart. In fact, the coexistence condition in terms of intensive variables requires that all phases must have equal temperature, pressure and chemical potentials of the M components. In the presence of polydispersity, one should thus solve a number of equations of the order of M^2 , a task which is practically impossible for M large or infinite.

However, the study of phase equilibria can conveniently start from the appropriate thermodynamic potential, which is the Helmholtz free energy A when the experimentally controlled variables are temperature, volume and numbers of different colloidal species. In the one-component case, the coexistence condition of

*Corresponding author. Email: gazzillo@unive.it

equal pressure and chemical potential has a simple geometrical interpretation in terms of free energy density a : the densities of two coexisting phases are determined by constructing a double-tangent to a plotted versus particle density. This recipe leads to the well known Maxwell construction, which connects suitably selected points along a van der Waals (vdW) subcritical isotherm, in order to 'reduce' its unphysical loop to a constant-pressure line characteristic of a first-order phase transition.

In the polydisperse case, a significant progress in the very difficult problem of predicting phase equilibria can be obtained for models with *truncatable* free energies (1). Here 'truncatable' means that the excess free energy of the polydisperse system turns out to depend only on a *finite* number of moments of the distribution corresponding to the polydisperse attribute (the diameter σ in the simplest cases). For spherical colloids, the excess free energy of the vdW model extended to polydisperse fluids has such a truncatable structure. Due to this property, this vdW theory has often been employed as the simplest model to investigate the effects of polydispersity on the gas-liquid transition (1; 2). On the other hand, the influence of polydispersity on freezing has been addressed by using the hard-sphere (HS) mixture model, which also admits a truncatable free energy (1) (for the fluid phase, the Boublik-Mansoori-Carnahan-Starling-Leland (BMCSL) (3) expression was employed). It is worth recalling that it is currently believed that size-polydispersity might destabilize crystallization, eventually inhibiting freezing above a certain 'terminal' value of polydispersity (1).

The present paper focuses on – and reviews – a number of recent attempts to investigate polydisperse phase equilibria, at least within some approximations, for another prototype model useful for studying colloidal suspensions, namely Baxter's sticky-hard-spheres (SHS) (4). Here the particles are hard spheres with a surface adhesion, and the corresponding potential can be obtained as a limit of an attractive square-well which becomes infinitely deep and narrow, according to a particular prescription which ensures a finite non-zero contribution of adhesion to the second virial coefficient ('sticky limit'). For the one-component version of this model, Baxter and collaborators (4) solved the Ornstein-Zernike (OZ) integral equation coupled with the Percus-Yevick (PY) approximation ('closure'). This *fully analytical* solution allows to determine all structural and thermodynamical properties of the SHS fluid. On the other hand, the multi-component PY solution, which soon followed Baxter's work (5; 6), is practically inapplicable in the presence of significant polydispersity. In fact, it requires the computation of a set of parameters $\{\Lambda_{ij}\}$ determined by a system of $M(M+1)/2$ quadratic equations, which – in general – cannot be solved even numerically for a mixture with a large number of components. Moreover, even in the presence of a general solution for this non-linear algebraic system, the problem of phase coexistence would still remain out of reach in view of the previous remarks.

In a series of recent papers (7; 8; 9; 11; 12; 13), we have attempted to make some progress along two different lines.

First, starting from the *density* expansion of the cavity function at contact, we have considered a sequence of simpler approximations (compared to the PY one) (7; 8; 9; 10; 11). Within the two simplest ones among these approximations, denoted as C_0 and C_1 (for reasons which will become clear in the following), we have been able to derive analytically all relevant information regarding structure and thermodynamics, including the phase coexistence, in view of the fact that the corresponding free energy turns out to be truncatable (11). Due to the simplicity of C_0 and C_1 , it is however reasonable to expect these approximations to fail at high packing fractions, with a consequently incomplete or even incorrect description of the effects of polydispersity on the phase diagram.

Therefore, in collaboration with Peter Sollich, we have recently explored a second approach (12), where the expansion variable (which must be small) is an appropriate polydispersity index. In such a way, we have tried to solve the non-linear algebraic system – involved in the PY result – *perturbatively in polydispersity*, starting from the monodisperse PY solution.

2 Baxter's SHS model and PY solution

The SHS model is defined as limiting case of a particular square-well (SW) model (4), based upon a potential including steeply repulsive core and short-ranged attractive tail, i.e.

$$\phi_{ij}^{\text{Baxter SW}}(r) = \begin{cases} +\infty & 0 < r < \sigma_{ij} \equiv (\sigma_i + \sigma_j)/2 \\ -\epsilon_{ij}^{\text{Baxter SW}} & \sigma_{ij} \leq r \leq R_{ij} \equiv \sigma_{ij} + w_{ij} \\ 0 & r > R_{ij} \end{cases} \quad (1)$$

with

$$\epsilon_{ij}^{\text{Baxter SW}} = k_B T \ln \left(1 + t_{ij} \frac{\sigma_{ij}}{w_{ij}} \right), \quad (2)$$

where σ_i is the HS diameter of species i , $\epsilon_{ij}^{\text{Baxter SW}} > 0$ and w_{ij} are the depth and the width of the well, respectively, k_B denotes Boltzmann's constant, T the temperature. Moreover,

$$t_{ij} = \frac{1}{12\tau_{ij}} \geq 0, \quad (3)$$

where the conventional Baxter parameter τ_{ij} is an unspecified increasing function of T , while τ_{ij}^{-1} measures the strength of surface adhesion or 'stickiness' between particles of species i and j .

The 'sticky limit' of $\phi_{ij}^{\text{Baxter SW}}(r)$ corresponds to taking $w_{ij} \rightarrow 0$. While the SW width goes to zero, its depth $\epsilon_{ij}^{\text{Baxter SW}}$ diverges, giving rise to a Dirac delta function in the Boltzmann factor (4), i. e.

$$e^{-\beta\phi_{ij}^{\text{SHS}}(r)} = \theta(r - \sigma_{ij}) + t_{ij} \sigma_{ij} \delta(r - \sigma_{ij}) \quad (4)$$

where $\beta = (k_B T)^{-1}$, while θ and δ are the Heaviside step function and the Dirac delta function, respectively.

The advantage of the sticky limit is that one effectively deals with a single parameter τ_{ij} for each pair, rather than a combination of energy and length scales (as occurs in the square-well model, for which no analytical solution is known). On the one hand, this particular limit has the disadvantage of introducing some pathologies in the model, notably in the one-component case (14). On the other hand, Baxter's model represents the simplest paradigmatic example of a combination of steep repulsion and short-range attraction which entails a complete analytical solution in the one-component case, within a robust approximation such as the PY closure.

In the multicomponent case, the PY solution of the OZ equation in terms of Baxter's factor correlation function reads (5; 6)

$$q_{ij}(r) = \begin{cases} \frac{1}{2}a_i(r - \sigma_{ij})^2 + (b_i + a_i \sigma_{ij})(r - \sigma_{ij}) + \Lambda_{ij}, & (\sigma_i - \sigma_j)/2 \leq r \leq \sigma_{ij} \\ 0, & \text{elsewhere,} \end{cases} \quad (5)$$

where the expressions for the parameters a_i and b_i may be found in (7), while the quantity

$$\Lambda_{ij} = t_{ij} y_{ij}(\sigma_{ij}) \sigma_{ij}^2, \quad (6)$$

which depends on the cavity function at contact $y_{ij}(\sigma_{ij})$, must be solution of the following system of quadratic equations

$$\Lambda_{ij} = \alpha_{ij} + \beta_{ij} \sum_m x_m \left[\Lambda_{im} \Lambda_{jm} - \frac{1}{2} (\Lambda_{im} \Gamma_{mj} + \Lambda_{jm} \Gamma_{mi}) \right], \quad i, j = 1, 2, \dots, M \quad (7)$$

Here, x_m is the molar fraction of the m -th species ($m = 1, \dots, M$), while $\alpha_{ij} = t_{ij} y_{ij}^{\text{HS-PY}}(\sigma_{ij}) \sigma_{ij}^2$, $\beta_{ij} = 12\rho t_{ij} \sigma_{ij}$ (ρ is the total number density), and $\Gamma_{ij} = \sigma_i \sigma_j / (1 - \eta)$, with η being the packing fraction (12). The solution of these equations for $\{\Lambda_{ij}\}$ is the real bottleneck of the multi-component PY result,

as mentioned in the Introduction: for large M (and in particular for $M \rightarrow \infty$) this calculation is next to impossible, neither analytically nor numerically.

As a consequence, although the PY closure is commonly believed to be very sound for short-range potentials (for one-component SHS fluids this was confirmed by recent numerical simulations (15)), one has to conclude that, in the multi-component (polydisperse) case, the PY solution has a very limited practical usefulness, since its solution scheme cannot be fully accomplished. This is the reason why other possible routes have been attempted, as we discuss next.

3 Simplified closures: the class of C_n approximations

A ‘closure’ is a relationship, added to the OZ equation, between the direct correlation function $c_{ij}(r)$ and $h_{ij}(r) = g_{ij}(r) - 1$ or $\gamma_{ij}(r) = h_{ij}(r) - c_{ij}(r)$ ($g_{ij}(r)$ being the radial distribution function) (16).

Let us go back to Baxter’s SW model given by Eq. (1) (i.e. *before* the ‘sticky limit’), and consider the following general class of ‘closures’ (10)

$$c_{ij}(r) = \begin{cases} -1 - \gamma_{ij}(r) & 0 < r < \sigma_{ij} \\ c_{ij}^{\text{shrink}}(r) & \sigma_{ij} \leq r \leq R_{ij} \\ 0 & r > R_{ij} \end{cases} \quad (8)$$

The expression $c_{ij}(r) = -1 - \gamma_{ij}(r)$ inside the core ($r < \sigma_{ij}$) is exact and dictated by the HS potential. The form outside the well ($r > R_{ij}$) may then be identified with the PY approximation,

$$c_{ij}^{\text{PY}}(r) = f_{ij}(r) [1 + \gamma_{ij}(r)], \quad (9)$$

since, for Baxter’s potential, the Mayer function, $f_{ij}(r) = \exp[-\beta\phi_{ij}(r)] - 1$, vanishes for $r > R_{ij}$.

The choice of $c_{ij}^{\text{shrink}}(r)$ inside the well (region which ‘shrinks’ in the sticky limit) defines one particular closure within the proposed class. Of course, $c_{ij}^{\text{shrink}}(r) = c_{ij}^{\text{PY}}(r)$ corresponds to the PY approximation. On the other hand, when $c_{ij}^{\text{shrink}}(r) \neq c_{ij}^{\text{PY}}(r)$, we are in the presence of *mixed closures*, which have frequently appeared in the literature (19). In order to define mixed closures simpler than the PY approximation, we consider the *density* expansion of the exact direct correlation function (16), and denote as C_n approximation a truncation of this series to order $O(\rho^n)$. The simplest two approximations are

$$\begin{aligned} c_{ij}^{\text{shrink}}(r) &= f_{ij}(r) & (C_0 \text{ closure}) \\ c_{ij}^{\text{shrink}}(r) &= f_{ij}(r) [1 + (\sum_k \rho_k f_{ik} * f_{kj})(r)] & (C_1 \text{ closure}), \end{aligned} \quad (10)$$

where ρ_k is the number density of species k , while $*$ denotes convolutive integration (10).

In the ‘sticky limit’ $R_{ij} \rightarrow \sigma_{ij}^+$ the well region shrinks, but a ‘memory’ of the approximation chosen for c_{ij}^{shrink} remains in the solution of the OZ integral equation. In fact, although all solutions $q_{ij}(r)$ corresponding to closures belonging to the class given by Eq. (8) have the same functional form as the PY solution – Eq. (5) –, each closure is characterized by its own approximation to $y_{ij}(\sigma_{ij})$, which is involved in the expressions of the parameters a_i , b_i , Λ_{ij} . For instance, the C_0 and C_1 approximations correspond to

$$\begin{aligned} y_{ij}(\sigma_{ij}) &= 1 & (C_0 \text{ closure}) \\ y_{ij}(\sigma_{ij}) &= 1 + y_{ij}^{(1)}(\sigma_{ij}) \eta & (C_1 \text{ closure}), \end{aligned} \quad (11)$$

which are, respectively, the zeroth- and first-order truncations of the density expansion for the exact cavity function at contact (see Ref. (10) for details).

While a brute-force truncation of the above-mentioned density expansions leads to analytical expressions simple enough to be applied to the multi-component (polydisperse) case, one should reasonably expect

less accuracy, expecially in the high-density regime. In the one-component case, we can carefully check this point.

In Figure 1 coexistence curves obtained from the C_0 and C_1 approximations are compared with the PY ones (using both compressibility and energy routes), and with Monte Carlo simulations from Ref. (15). It is apparent how the PY energy route (PYE) yields a rather precise representation of the MC results, unlike the compressibility route (PYC). It is worth noting that the results stemming from the C_1 approximation, although rather close to the MC data in the low-density branch, clearly fail to accurately reproduce them for higher densities, as expected.

In spite of their lack of accuracy, the C_0 and C_1 approximations provide however a rather sound basis for getting some insight into phase equilibria of polydisperse SHS fluids, since they allow simple analytical, or semi-analytical, treatments.

A first important feature of the C_0 and C_1 approximations for polydisperse SHS is that the corresponding free energy has a *truncatable* structure, that is it depends upon few (4 at most) moments of the (discrete) size distribution, $\xi_\nu = (\pi/6)\rho \sum_j x_j \sigma_j^\nu$ with $\nu = 0, 1, 2, 3$.

A second remarkable fact is that the C_0 and C_1 approximations are able to describe the so-called *fractionation* phenomena characteristic in phase equilibria of polydisperse systems. While we refer to a recent review (1) for detailed description of the increased complexity in the polydisperse phase diagrams, here we just mention the two important points. First, fractionation means that daughter phases, obtained from demixing of a parent homogeneous phase, need not have the same composition of the parent phase. As a consequence, there is no a single coexistence line ('binodal') as in the one-component case, but one rather finds a *cloud curve*, representing the temperature-density dependence line of the low-density majority phase ('gas'), and a *shadow curve* representing the temperature-density dependence of the high-density minority phase (incipient 'liquid'). While for one-component systems these two curves are identical, for polydisperse systems in general they are not, with the exception of the critical point where they coincide by definition.

However, in order to apply the C_0 and C_1 approximations to the multi-component SHS model, we have to tackle a further important problem, that is the definition of the stickiness parameters τ_{ij} .

4 Size-dependence of stickiness parameters

In mixtures, τ_{ij} will depend on the particular pair i, j considered, and reasonably should be expected to be related to the particles sizes. Assuming that we are dealing only with size-polydispersity, we can always decouple temperature and adhesion as

$$\frac{1}{\tau_{ij}} = \frac{1}{\tau} \epsilon_{ij} = \frac{1}{\tau} \mathcal{F}(\sigma_i, \sigma_j) \quad (12)$$

where the last equality stems from the assumption of size-polydispersity and of a purely pairwise potential. Unfortunately, the exact form of the size-dependence of these stickiness parameters is still an open problem, due to the lack of experimental and theoretical insights on this (13). On the other hand, few guidelines – based on arguments discussed in Refs. (11; 12) – provide, as reasonable and plausible, the following dependences

$$\epsilon_{ij} = \mathcal{F}(\sigma_i, \sigma_j) = \begin{cases} \sigma_0^2/\sigma_{ij}^2 & \text{Case I ,} \\ \sigma_i \sigma_j / \sigma_{ij}^2 & \text{Case II ,} \\ 1 & \text{Case IV ,} \\ \sigma_0 / \sigma_{ij} & \text{Case V .} \end{cases} \quad (13)$$

Here σ_0 is a characteristic reference length (e.g. the parental mean diameter) and the numbering of the various cases follows the convention of previous work (11; 12).

Figure 2 reports the results of the calculation of the cloud and shadow curves for polydisperse SHS within the simple C_0 approximation. Here and below, polydispersity is measured by an index s , which is the normalized standard deviation of the size distribution. Hence $s = 0$ corresponds to a mono-disperse

case, whereas $s = 0.1$ and $s = 0.3$ indicate moderate and significant polydispersity, respectively. The top panel of Fig. 2 depicts the results for case I of size-dependence of stickiness parameters. As s increases, the coexistence region shrinks, thus suggesting that polydispersity *disfavours* the phase transition. On the other hand, this trend is markedly case-dependent, as illustrated in the bottom panel of Fig. 2, where the cloud-shadow pairs with polydispersity $s = 0.3$ are displayed for different cases of size-dependence. It can be clearly seen that while, for cases I and V the same trend is observed, case IV seems to suggest a *widening* of the phase coexistence region (and hence a favouring of the phase transition).

In view of the lack of numerical simulation for polydisperse SHS to compare with, we have no way, at the present stage, to check how realistic those results are. On the other hand, we might suspect, based on the comparison in the one-component case, C_0 to fail to provide accurate representation in the region of low temperatures and high densities. This is the reason why other possible approaches have been recently tested. We now illustrate a different perturbative approach, which has proved to be promising in this context.

5 Perturbative treatment of the SHS-PY solution

The main difficulty in dealing with the PY solution for polydisperse SHS stems from the solution of the coupled quadratic system of equations (7), as remarked. As the one-component case has a well-defined solution, one might then suspect that – for weak polydispersity – a perturbative expansion around this solution might include the main effects of polydispersity. This is in fact what happens, as recently shown (12) by exploiting a general perturbation theory due to Evans (17). The main idea is that, for weak polydispersity, size-distributions are narrowly peaked around a mean reference value (σ_0 in the present case), and hence all quantities such as

$$\delta_i = \frac{\sigma_i - \sigma_0}{\sigma_0} \ll 1, \quad (14)$$

are small. Therefore one might expand both ϵ_{ij} , and all quantities appearing in Λ_{ij} , in powers of δ_i . Similar expansion can be performed in the free energy, and hence all thermodynamic quantities can be computed. The entire procedure is described in detail in Refs. (1; 12; 17). Here we just summarize the main results.

The approximate range of validity of the perturbation expansion can be envisaged by considering the polydisperse HS case where the ‘exact’ BMCSL approximation (3) can be compared with the corresponding perturbative solution based on the one-component ($s = 0$) counterpart. This is reported in the top-left part of Figure 3, where the quantity $\beta P v_0$ ($v_0 = \pi \sigma_0^3/6$) is plotted against the packing fraction η for increasing values of polydispersity. It is apparent how the perturbative solution remains rather close to the ‘exact’ polydisperse BMCSL solution even for moderate polydispersity $s \leq 0.3$, which is the maximum value considered in the remaining part of the work. The remaining plots in Figure 3 display the effect of polydispersity on the PY pressure equation of state as obtained from the energy route and for decreasing values of the temperature τ . In the one component case $s = 0$, a van der Waals loop starts to appear when we cross the critical temperature $\tau_c \sim 0.1185$ coming from the high τ regime. Obviously this signals the onset of a liquid-gas phase transition, and the corresponding phase diagram can be obtained by a standard Maxwell construction by connecting appropriate points with the same pressure. In the presence of polydispersity (here represented by choice IV for size-dependence of the stickiness parameters) the same procedure *cannot* be applied due to fractionation, as already discussed. Nevertheless, we can clearly see that as s increases, the van der Waals loop region (when present) expands, thus suggesting that phase transition is favored by the presence of polydispersity. A similar feature occurs for the polydisperse van der Waals model (2) and for the numerical results of the PY compressibility equation of state (18) (note that in the latter a *gap* rather than a *loop* is signalling the onset of the transition). A somewhat surprising feature is that, at fixed packing fraction η , the pressure decreases with increasing polydispersity *less* in the presence of adhesion rather than in its absence (i.e. for the HS case). An intuitive plausible interpretation of this feature can be found in Ref. (12).

The same perturbative approach allows the determination of the cloud and shadow curves for the various

cases of size-dependence of τ_{ij}^{-1} . This is reported in Figure 4 for cases II, IV (top panel) and I, V (bottom panel). In the first case the cloud and shadow lines collapse into a single curve, and this can be understood on the basis of the particular scaling properties of the free energy to this order in perturbation theory (12). In all cases there is a breakdown of the perturbation theory on approaching the critical point, and this is a known general drawback of Evans' perturbative scheme. Nevertheless, in all cases and to this order in perturbation theory, there is a tendency of the phase coexistence region to *increase* with polydispersity, in qualitative agreement with the intuitive picture obtained from Figure 3.

It is worth stressing the difference with previous non-perturbative results stemming from the C_0 solution, where all different cases (with the notable exception of IV) were predicting a reduction of the phase coexistence region. While in the C_0 description we have provided a careful treatment of polydispersity at the expenses of accuracy of the exploited approximation, in the perturbative description of the PY solution, polydispersity is assumed to be small and hence one might suspect that solutions with large polydispersities cannot fit within this picture. On a balance, nevertheless, we would favour the latter rather than the former description. An almost correct representation of the one-component counterpart, is a necessary requirement to check the effect of polydispersity on it, and we are not aware of any physical or experimental system where the effects of polydispersity are so strong that they could not kept into account, at least at the simplest qualitative level, by the perturbative scheme proposed here. Along this line, some further proposals have been put forward in Ref. (12) to derive a phenomenological BMCSL-like approximation for SHS, which might be regarded as our 'best and simplest guess' to the *exact* phase behavior of polydisperse SHS. Even on the size-dependence of τ_{ij}^{-1} some possible support of the proposed forms may be argued (12; 13).

6 Conclusions

In this work we have summarized recent advances in predicting theoretically the phase diagram for polydisperse suspensions of colloidal particles with surface adhesion, within the simple description of Baxter's model. Emphasis was put on the crucial – unsolved – step required to get the multi-component SHS-PY solution, and the proposed recipes to deal with this problem. This first one is based on a simplification of the closure. It has the advantage of allowing a complete analytical analysis on the effects of polydispersity, including fractionation, but has the disadvantage of a very questionable accuracy. The second one is based on a perturbative method, starting from the energy PY one-component solution, which is known to provide an accurate description of the phase diagram. The drawback of this scheme is that it works for mild polydispersity, and that cannot describe the changes of the critical point region. Notwithstanding these limitations, this novel approach is expected to find practical application in the interpretation of all those phenomena where Baxter's model and polydispersity both play a privileged role.

Acknowledgments

Part of the work appearing here has been obtained in collaboration with Peter Sollich.

References

- [1] P. Sollich, *J. Phys.: Condens. Matter* **14** R79 (2002).
- [2] L. Bellier-Castella, H. Xu and M. Baus, *J. Chem. Phys.* **113**, 8337 (2000)
- [3] T. Boublík, *J. Chem. Phys.* **53**, 471 (1970); G. A. Mansoori, N. F. Carnahan, K. E. Starling and T. W. Leland Jr, *J. Chem. Phys.* **54**, 1523 (1971); J. J. Salacuse and G. Stell, *J. Chem. Phys.* **77**, 3714 (1982).
- [4] R. J. Baxter, *J. Chem. Phys.* **49**, 2270 (1968). R. J. Baxter, in: *Physical Chemistry, an Advanced Treatise*, Vol. 8A, ed. D. Henderson (Academic Press, New York, 1971) ch. 4. R. O. Watts, D. Henderson and R. J. Baxter, *Advan. Chem. Phys.* **21**, 421 (1971).
- [5] J. W. Perram and E. R. Smith, *Chem. Phys. Lett.* **35**, 138 (1975).
- [6] B. Barboy and R. Tenne, *Chem. Phys.* **38**, 369 (1979).

- [7] D. Gazzillo, and A. Giacometti, *J. Chem. Phys.* **113**, 9837 (2000); ibidem *Physica A*, **304**, 202 (2002).
- [8] D. Gazzillo, and A. Giacometti, *Mol. Phys.* **100**, 3307 (2002).
- [9] D. Gazzillo, and A. Giacometti, *Mol. Phys.* **101**, 2171 (2003)
- [10] D. Gazzillo, and A. Giacometti, *J. Chem. Phys.* **120**, 4742 (2004).
- [11] R. Fantoni, D. Gazzillo, and A. Giacometti, *J. Chem. Phys.* **122**, 034901 (2005); ibidem *Phys. Rev. E* **72**, 011503 (2005).
- [12] R. Fantoni, D. Gazzillo, A. Giacometti, and P. Sollich, *J. Chem. Phys.* (2006), in press.
- [13] D. Gazzillo, A. Giacometti, R. Fantoni, and P. Sollich, *Phys. Rev. E.* (2006), in press.
- [14] G. Stell, *J. Stat. Phys.* **63**, 1203 (1991).
- [15] M. A. Miller, and D. Frenkel, *Phys. Rev. Lett.* **90**, 135702 (2003); ibidem, *J. Chem. Phys.* **121**, 535 (2004). ibidem, *J. Phys. Cond. Mat.* **16**, S4901 (2004).
- [16] J. L. Barrat, and J. P. Hansen, *Basic Concepts for Simple and Complex Liquids* (Cambridge University Press, Cambridge) (2003); J. P. Hansen and I. R. Mc Donald, *The Theory of Simple Liquids* (Academic, London) (1986).
- [17] M. L. Evans, *J. Chem. Phys.* **114**, 1915 (2001)
- [18] C. Robertus, W.H. Philipse, J.G. Joosten, and Y. K Levine, *J. Chem. Phys.* **90**, 4482 (1989)
- [19] J. N. Herrera and L. Blum, *J. Chem. Phys.* **94**, 5077 (1991)

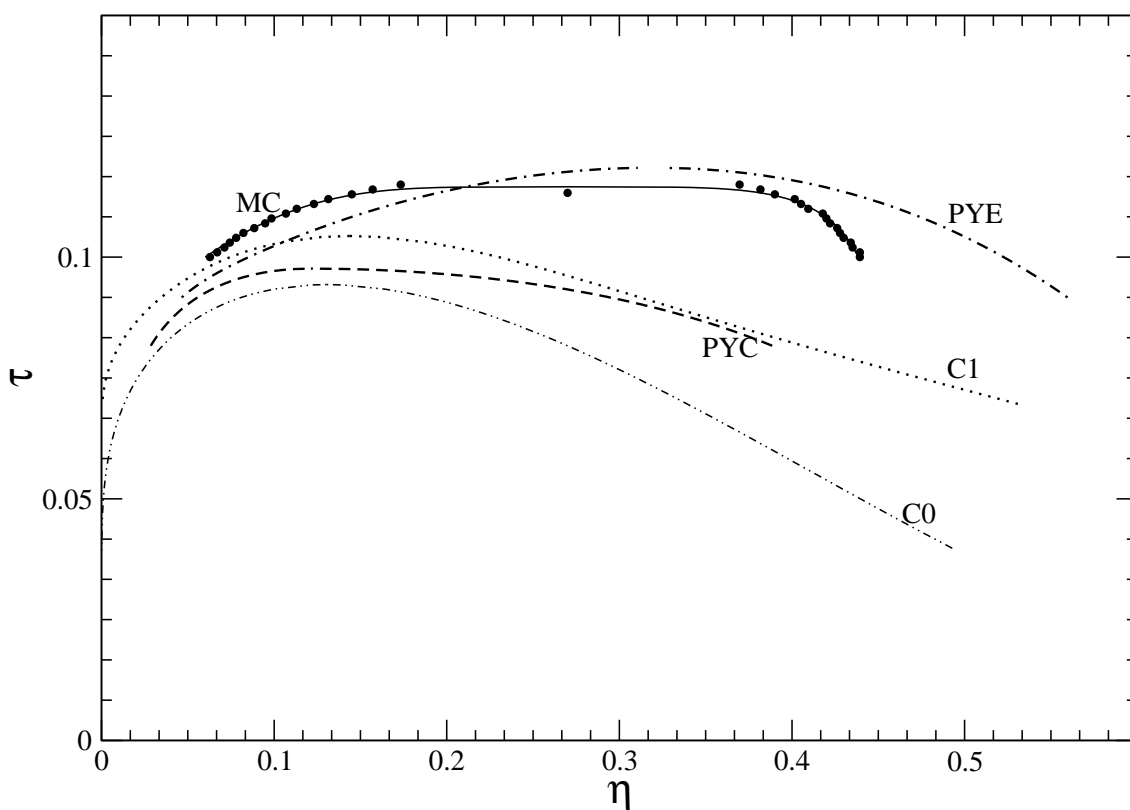


Figure 1. Coexistence (binodal) curves for the one-component Baxter model. Both compressibility (PYC) and energy (PYE) equation of state as obtained from the Percus-Yevick approximation (see Ref (4)) are reported and compared with C_0 and C_1 approximations from Ref. (11) and with Monte Carlo simulation (MC) from Ref. (15). In the MC case the continuous line is simply a guide to the eye.

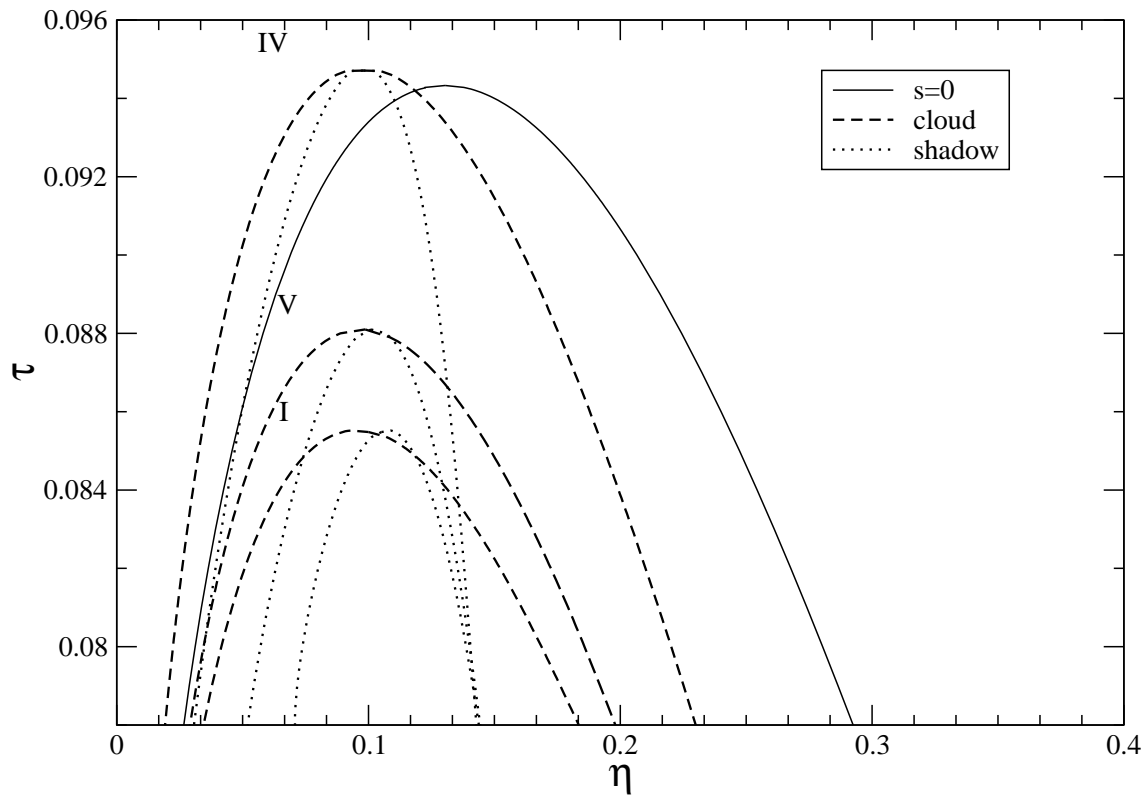
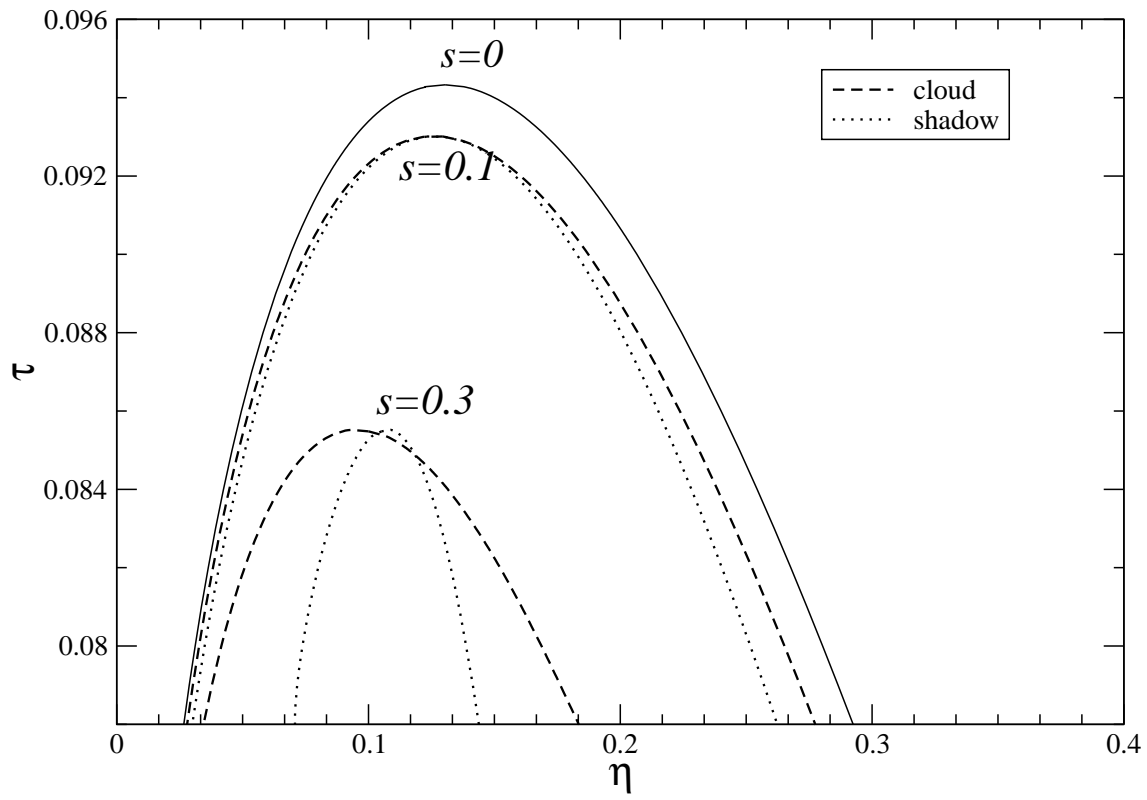


Figure 2. (Top) Cloud and shadow curve for model I within the C_0 approximation at increasing polydispersity: $s = 0$, $s = 0.1$ and $s = 0.3$. (Bottom) Same as above for fixed value of polydispersity $s = 0.3$ and different choice of the stickiness adhesion (model I, IV and V)

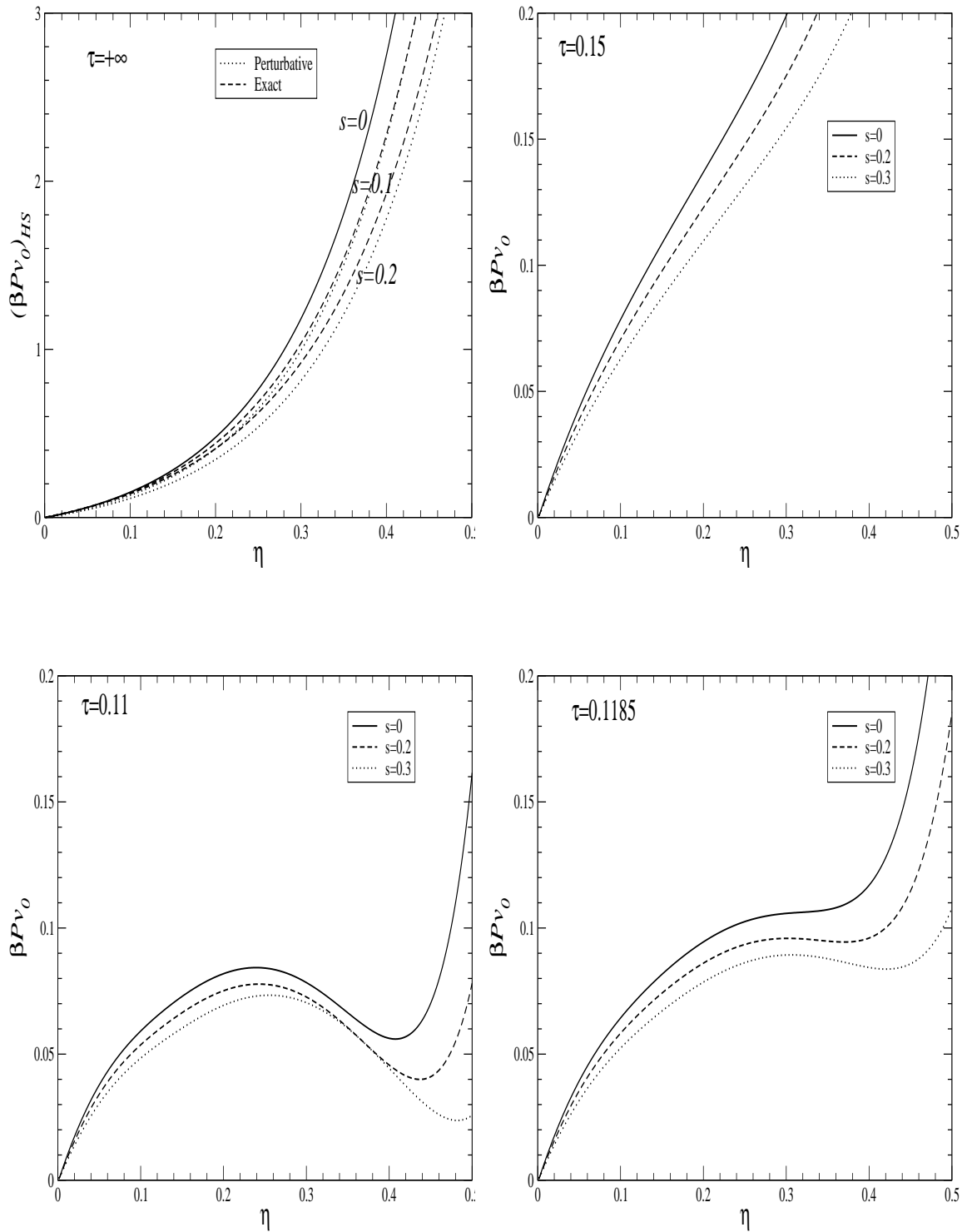


Figure 3. Behavior of the energy equation of state within our perturbative scheme. In all cases the quantity $\beta P v_0$ is plotted against the packing fraction η . In clockwise order, the first curve (left, top) reports a comparison of the perturbative versus the 'exact' BMCSL solution in the equation of state for polydisperse HS ($\tau = +\infty$). The other curves report the perturbative solution for the energy equation of state within the PY approximation for SHS Baxter model. Results are depicted for three values of temperature $\tau = 0.15 > \tau_c$, $\tau = 0.1185 \sim \tau_c$ and $\tau = 0.1 < \tau_c$ and for different degrees of polydispersity. The choice for the size-dependence of stickiness parameters corresponds to model IV.

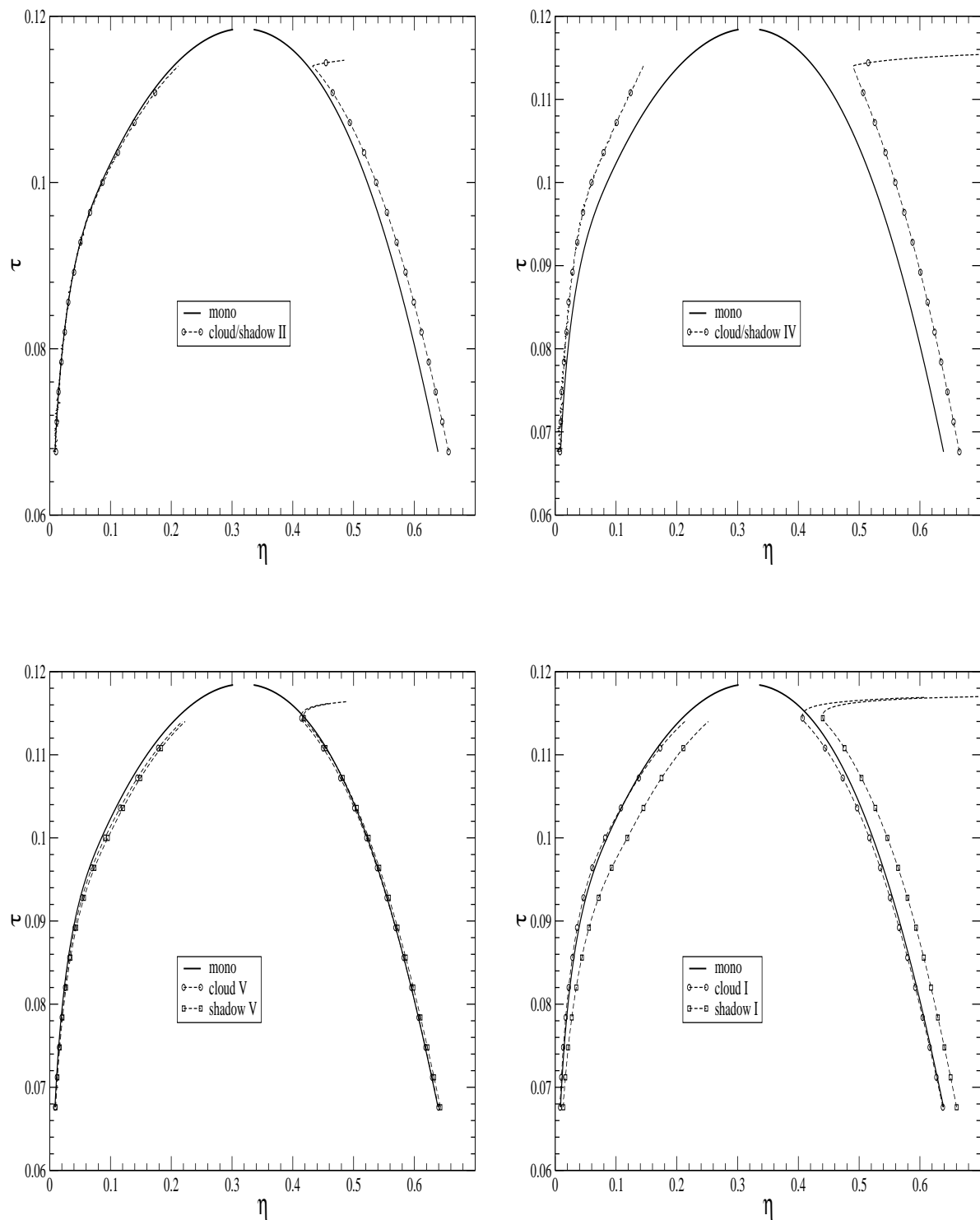


Figure 4. Cloud/Shadow pairs from the perturbative results for the PY solution of SHS Baxter model. In clockwise order the results for choices II, IV (top) and I, V (bottom) are depicted. In the two top panels, the cloud and shadow curves coincide to this order in perturbation, whereas in the bottom panels they are different. In order to have all pictures on the same scale, the selected value for polydispersity is $s = 0.3$ for models II, IV (top) and $s = 0.1$ for models I, V (bottom). In all cases the continuous curve represents the monodisperse ($s = 0$) result.